Twentieth century North Atlantic jet variability

Tim Woollings,[a]* Camelia Czuchnicki[a] and Christian Franzke[b]
[a]Department of Meteorology, University of Reading, UK
[b]British Antarctic Survey, Cambridge, UK

*Correspondence to: T. Woollings, Department of Meteorology, University of Reading, Earley Gate, PO Box 243, Reading, RG6 6BB, UK. E-mail: t.j.woollings@reading.ac.uk

Long records of the latitude and speed of the North Atlantic eddy-driven jet stream since 1871 are presented from the newly available Twentieth Century Reanalysis. These jet variations underlie the variability associated with patterns such as the North Atlantic Oscillation (NAO) and have considerable societal impact through variations in the prevailing westerly winds. While the NAO combines variations in the latitude and speed of the jet, these two characteristics are shown to have quite different seasonal cycles and interannual variability, suggesting that they may have different dynamical influences.

In general, the features exhibited in shorter records are shown to be robust, for example the strong skewness of the NAO distribution. Related to this is a clear multimodality of the jet latitude distribution, which suggests the existence of preferred positions of the jet. Decadal variations in jet latitude are shown to correspond to changes in the occurrence of these preferred positions. However, it is the speed rather than the latitude of the jet that exhibits the strongest decadal variability, and in most seasons this is clearly distinct from a white-noise representation of the seasonal means. When viewed in this longer term context, the variations of recent decades do not appear unusual and recent values of jet latitude and speed are not unprecedented in the historical record.

Key Words: jet variability; NAO; reanalysis; climate noise; regime behaviour

Received 11 September 2012; Revised 14 May 2013; Accepted 15 May 2013; Published online in Wiley Online Library

1. Introduction

The midlatitude eddy-driven jet streams are manifested at the surface as prevailing westerly winds, and as such their variability has considerable societal impact. In the North Atlantic, the eddy-driven jet is variable on all time-scales from days to decades and this variability is partly described by patterns such as the North Atlantic Oscillation (NAO), Northern Annular Mode (NAM) and East Atlantic (EA) pattern (e.g. Athanasiadis *et al.*, 2010). Over recent decades, the jet variations described by the NAO/NAM in particular have driven anomalous patterns of temperature, precipitation and storm activity around the Atlantic basin and beyond (Hurrell, 1995; Thompson and Wallace, 2001; Hurrell and Deser, 2009). The change from extreme negative to positive NAO values between the 1960s and 1990s continues to provoke much discussion, despite the more recent return to moderate and negative values (Cohen and Barlow, 2005; Cattiaux *et al.*, 2010).

North Atlantic variability has been extensively described over the second half of the 20th century using reanalysis products that assimilate both surface and upper-air observations. Prior to this, some information on NAO variations, for example, has been inferred from surface-pressure reconstructions or station data (Jones *et al.*, 1997; Luterbacher *et al.*, 2001; Pinto and Raible, 2012). In a recent advance, the Twentieth Century Reanalysis project (Compo *et al.*, 2011) assimilated only surface observations in deriving dynamically consistent three-dimensional fields back to the late 19th century. This provides an opportunity to analyze the characteristics of jet variability in an observationally constrained dataset of unprecedented length. For the purpose of evaluating climate models, it is useful to determine whether jet characteristics derived from recent decades are robust features of a longer record.

In this article we analyze the variability of the latitude and speed of the North Atlantic eddy-driven jet stream in the Twentieth Century Reanalysis. These quantities have been derived from the near-surface zonal wind field following the method of Woollings *et al.* (2010a) and can be related in particular to changes in the NAO and EA (Woollings *et al.*, 2010a; Woollings and Blackburn, 2012). Some studies have diagnosed jet variations and trends in the recent reanalysis period (Strong and Davis, 2007, 2008; Archer and Caldeira, 2008; Franzke and Woollings, 2011) and one of the key aims of this study is to put these in the context of a longer observational record. A more general aim is to assess the level of jet variability on decadal time-scales. One previously unexplored aspect of this is whether the level of intraseasonal jet variability itself exhibits long-term changes in magnitude. This question was inspired by the recent suggestion of Häkkinen *et al.* (2011) of multi-decadal variations in the frequency of Atlantic/European blocking. We also take this opportunity to describe the seasonal cycles of the jet quantities and their variations between different periods.

© 2013 Royal Meteorological Society

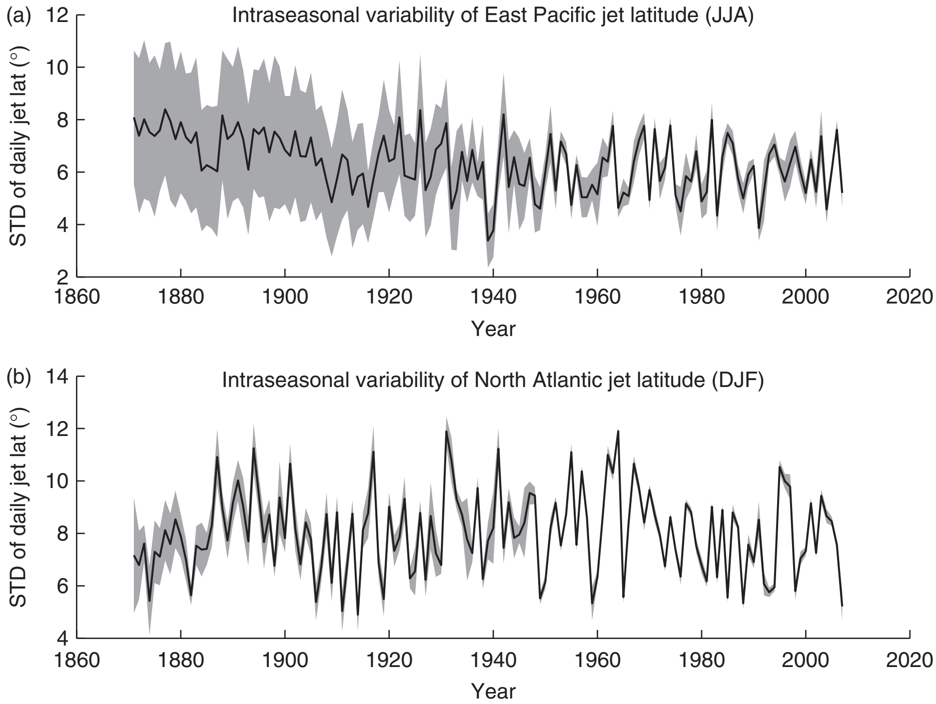

Figure 1. Time series of the intraseasonal variability of the jet speed. This series is formed by taking the standard deviation of the 90 days in each individual season. Shading shows the ±2 standard deviation range across the ensemble. (a) Eastern North Pacific (200–240°E) JJA; (b) North Atlantic (0–60°W) DJF.

2. Methodology

Woollings *et al.* (2010a) used zonal wind averaged over 925–700 hPa to derive daily indices of jet latitude and speed. On testing, it was found that almost identical results were obtained using only the 850 hPa values (Czuchnicki, 2011), so only this level was used for simplicity and to reduce data requirements. The method consists of zonally averaging the zonal wind over the sector 0–60°W in the North Atlantic, then applying a 10 day low-pass filter before simply identifying the maximum westerly wind speed within the range 15–75°N. The location and size of this value are used to define the daily jet latitude and speed respectively. No interpolation is used, so the jet indices have the reanalysis resolution of 2° in latitude. In contrast to Woollings *et al.* (2010a), we do not remove the seasonal cycles of the jet indices; these are instead retained for analysis.

The 10 day low-pass filter acts to remove some short time-scale noise but does not dramatically change the wind field, since the longitudinal mean also acts to remove short time-scales (see figure 3 of Woollings *et al.* 2010a). Therefore, while the indices have a daily time resolution, they effectively measure variations in slowly varying weather regimes with periods of 10 days or longer. In section 6, we then average the daily series up to seasonal means to study the interannual and decadal variability of the jet. This step enables us to consider the interannual–decadal variability separately for each season, motivated by the expectation that different processes may act as external influences in each season. Note that this approach also averages over the considerable structure in the jet latitude distribution although, in order to summarize the position of the jet in any season with one number, this seems unavoidable.

Note that these simple diagnostics measure the basin-scale westerly winds and as such should be considered as physical indicators of the flow variability associated with large-scale phenomena such as the NAO. By using zonal wind in the lower troposphere, the diagnostics isolate the part of the large-scale flow that is driven by transient baroclinic eddies. Instantaneous flow fields over the Atlantic can often exhibit considerable meridional structure, which is averaged over in this method. Other indices have been developed to track these structures (Koch *et al.*, 2006; Limbach *et al.*, 2012). One feature of this method is that it defines values for the jet latitude and speed on every single day. On occasions when the jet is split into two branches, only the strongest of these is considered. In the average over 0–60°W such splits are rare and a unique westerly jet is almost always clear, as shown by the example winter Hovmöller diagrams in figure 1 of Hannachi *et al.* (2012). Similar results are also seen in other seasons (not shown).

Daily data from the Twentieth Century Reanalysis of Compo *et al.* (2011) has been used for the period February 1871–January 2008, which gives a sample size of 136 full winter seasons and 137 of each of the other seasons. One of the novel aspects of the Twentieth Century Reanalysis is the use of an ensemble method to provide information on the uncertainty. In regions and periods of sparse observational coverage, the model is insufficiently constrained by the observations, resulting in spread between the ensemble members. Here we use this ensemble information to provide uncertainties in the jet diagnostics, simply by repeating the analysis for each of the 56 ensemble members and presenting ranges of each diagnostic across the ensemble.

3. A cautionary example

In this article we focus exclusively on the North Atlantic, partly because of its dynamical significance but also because of the relatively good observational coverage. Similar analyses have been performed for other regions (Czuchnicki, 2011) but in these cases the conclusions are limited, due to ensemble spread and the associated uncertainty in the early period of the reanalysis. In this section we show one example of these analyses, which illustrates that particular care needs to be taken over apparent trends exhibited in this early period.

Figure 1(a) shows the time series of summertime intraseasonal variability of jet latitude in the eastern North Pacific. The intraseasonal variability is defined here as the standard deviation of the jet indices in each 90 day season. In the Pacific case, there is an apparent long-term trend of decreasing intraseasonal variability. However, much of this trend occurs in the period before 1940 when the large ensemble spread reflects insufficient observational coverage to constrain the model. It is likely that this trend in fact reflects a drift of the model back towards its unconstrained state, which seems to be biased towards overly variable jet speeds. The use of the ensemble information has

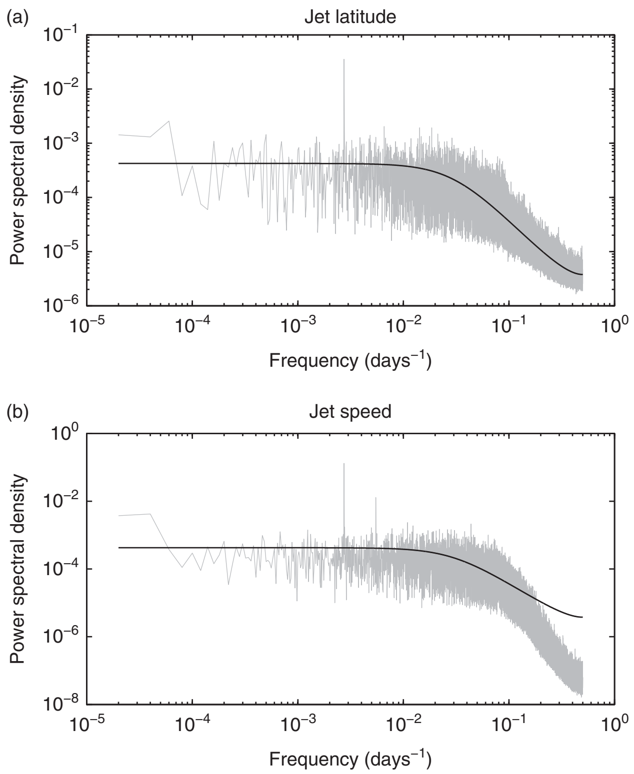

Figure 2. Spectra of (a) North Atlantic jet latitude and (b) speed. The black lines indicate the theoretical spectra of the corresponding AR1 process derived from the variance and lag-1 autocorrelation of the series. Note that leap days have been neglected for this figure.

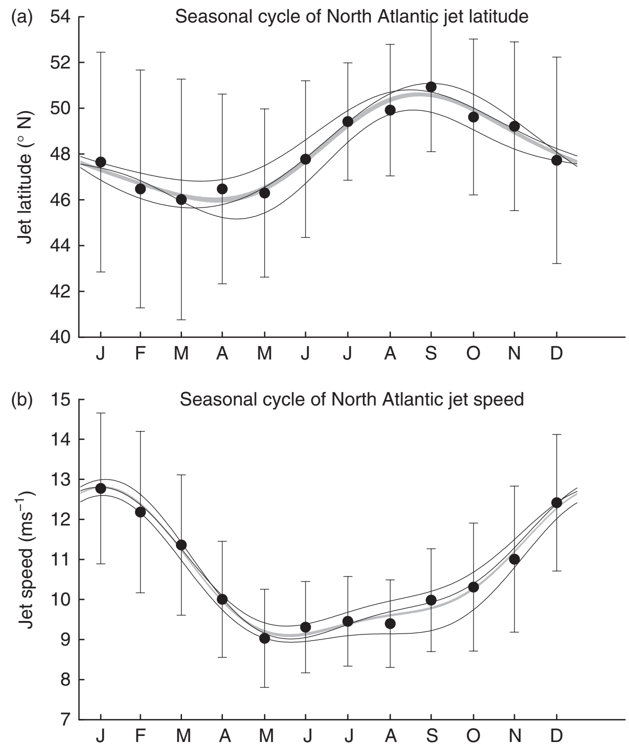

Figure 3. Seasonal cycles of (a) jet latitude and (b) speed, shown at both daily and monthly time resolution. The seasonal cycles are derived by averaging the jet indices over all complete years of the reanalysis. The daily resolved cycles are shown by the grey shading, which indicates the ± 2 standard deviation range across the 56 ensemble members. The individual black lines show the daily cycles exhibited by subsamples of three non-overlapping 45 year periods. Black dots mark the monthly averages of the ensemble mean data, with bars indicating ranges of ± 1 standard deviation across the 136/7 months of the record. The daily resolved versions have been smoothed in frequency space by retaining only the two lowest frequencies. This smoothing accounts for the small discrepancies between the monthly and daily resolved versions.

helped to identify this problem and this shows that misleading results could be obtained when only the ensemble mean is used.

An example of the same diagnostic is given for the North Atlantic in Figure 1(b). In this case the range between ensemble members is much smaller, so that the existence of decadal-scale variations in the level of variability can be identified with reasonable confidence. (These are in fact the variations that we focus on in section 7). However, although the spread is much smaller, the possibility of this effect contributing to some early variations should not be ruled out.

4. Spectral characteristics and seasonal cycles of the North Atlantic jet

Figure 2 shows spectra of the raw jet latitude and speed indices. The spectrum of jet latitude in Figure 2(a) is generally similar to the theoretical spectrum of the corresponding red-noise process (shown by the black line). There is, however, a clear peak at a period of 365 days (frequency $2.7 \times 10^{-3}\,\mathrm{d}^{-1}$) indicating the presence of a seasonal cycle. The spectrum of jet speed in Figure 2(b) is less similar to the corresponding red-noise process, in particular with less power at periods shorter than 10 days. This contrast may arise from the nature of the jet definitions, in which the latitude in particular can change rapidly between one day and the next as one pulse of westerly wind is replaced by a stronger wind feature at a different latitude. The jet speed spectrum also has a peak at 365 days and another clear peak at 182.5 days, showing that the second harmonic is also required to describe the seasonal cycle in this case. Both spectra show high power at the lowest frequencies. This is investigated further in section 6 on a season-by-season basis, as it is anticipated that different mechanisms might lead to interannual–decadal variability in different seasons.

Osprey and Ambaum (2011) recently showed that the Northern Annular Mode exhibits exponential power spectra at periods shorter than 36 days, indicative of chaotic behaviour. Interestingly, the spectra shown in Figure 2 do not fit an exponential decay particularly well, an impression that is confirmed when the spectra are replotted with a linear x axis (not shown). This difference may arise from the nature of the jet diagnostics, in which wind maxima are sought in low-pass filtered data, or from the regional rather than hemispheric focus taken here.

The seasonal cycles themselves are shown in Figure 3. The general shape of these is as expected from the changes in temperature gradients, with the jet strengthening and moving equatorward during winter. The jet latitude cycle shows considerable lag with respect to the insolation, with the jet at its equatormost point in March–May rather than the conventional December–February winter season. The jet proceeds poleward during the summer and reaches its maximum latitude in September. Although the seasonal cycle emerges clearly in both this and the spectral analysis, it is in fact rather small, with the jet moving only around 5° over the year. This variation is much smaller than the month-to-month variability, as shown by the vertical bars. For example, there are clearly many examples of winter months when the jet position has been further poleward than the average summer monthly position. This is consistent with the dominance of time-scales shorter than a year in the temporal variance of the jet latitude index (Franzke and Woollings, 2011).

The seasonal cycle of jet speed is more pronounced compared with the variability, although there are clearly still many winter months with jet speeds as weak as those typically seen in summer. The contribution of the semi-annual period acts to add an asymmetry to the cycle, so that the jet rapidly weakens from its strongest in January to its weakest in May. It is not clear what physical processes lie behind this asymmetry.

The seasonal cycles of three 45 year subsets are also shown in this figure. These show that there can be considerable differences in the shape of the cycles between different periods, which can give different impressions of the symmetry, for example. The

© 2013 Royal Meteorological Society

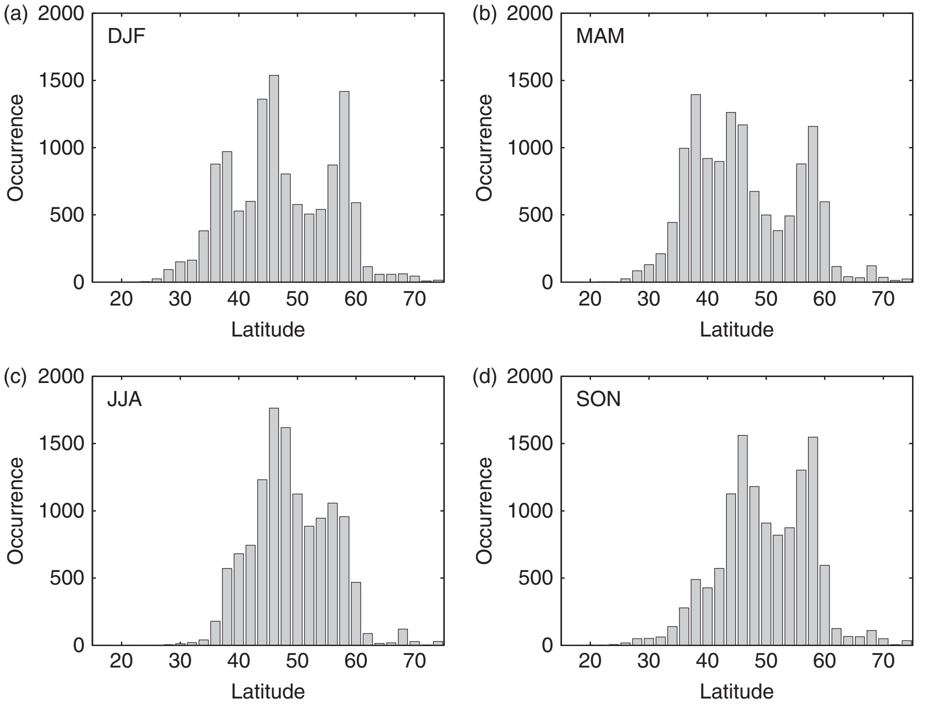

Figure 4. Ensemble means of the distribution of jet latitude in the four seasons (the distributions are calculated for each ensemble member and then averaged). The standard deviation between the ensemble members is typically only 20–30 occurrences on the scale used here, so is not shown.

notion of convergence is somewhat ill-founded in the presence of time-varying forcings, but this does suggest that even periods as long as the ERA-40 reanalysis, for example, may not be definitive for the purpose of assessing the climatology of a numerical model.

5. Jet index distributions

Woollings *et al.* (2010a) showed that in the ERA-40 reanalysis the distribution of the jet latitude index in North Atlantic winter exhibits a trimodal structure, which could reflect the existence of distinct flow regimes (see also Franzke *et al.*, 2011; Hannachi *et al.*, 2012). We present the same analysis for the Twentieth Century Reanalysis data in Figure 4. In winter this shows a very similar trimodal structure to that seen in ERA-40. This supports the robustness of this distribution and shows that it is not an accident of the most recent few decades. The other seasons show more structure in the distributions than seen in ERA-40, with some evidence of preferred flow regimes in spring and autumn in particular. Interestingly, the locations of these seem very similar in the different seasons, which suggests that the occurrence of preferred jet positions may be related to the location of physical features such as orography, coastlines or ocean currents.

The jet latitude can be considered as a physical interpretation of NAO variability, and Woollings *et al.* (2010b) investigated the non-Gaussian structure of the NAO distribution in the ERA-40 reanalysis as part of the jet variability. It is of interest, then, to verify whether this non-Gaussian NAO structure is also evident in the long 20CR record. Figure 5 shows the structure of winter NAO variability as derived from the leading Empirical Orthogonal Function (EOF) of monthly mean sea-level pressure. The NAO distribution is strongly negatively skewed, supporting the results found in the shorter record.

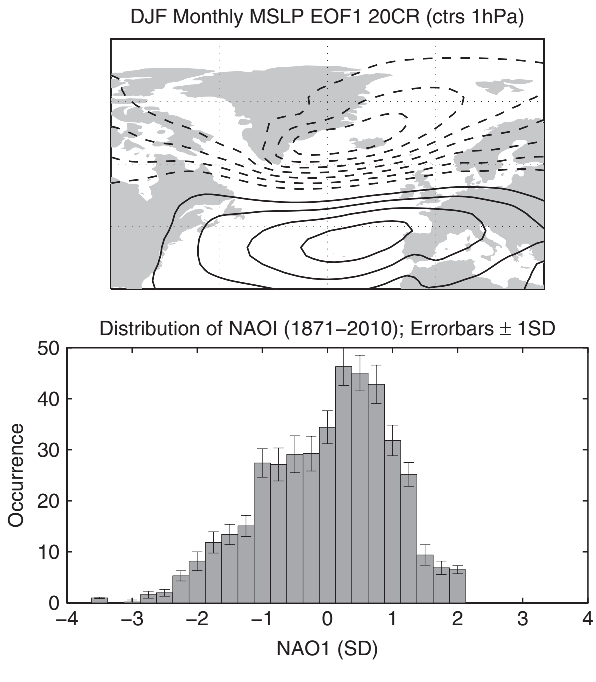

Figure 5. Structure of NAO variability in the 20CR reanalysis. The top panel shows the ensemble mean NAO pattern, defined as the leading EOF of monthly mean sea-level pressure over the region shown. The contour interval is 1 hPa, with negative contours dashed and the zero contour omitted. The lower panel shows the ensemble mean distribution of the corresponding principal component, with error bars indicating the ±1 standard deviation range across the ensemble.

Figure 6(a) shows the variability of the wintertime distribution between individual 20 year periods. In general, each of the three peaks in the distribution is represented at the same location in each of the periods, although the southern jet position was particularly rare in both the 1870s/80s and 1990s/2000s. This figure gives the impression that decadal jet variability is associated with low-frequency changes in the occurrence of each of the three fixed jet positions. Such decadal-scale variations in the occurrence frequencies of the three distinct jet regime states have been reported in the shorter ERA-40 record by Franzke *et al.* (2011). This impression is further confirmed by Figure 6(b), which summarizes the variability in the shape of the Probability Density Function (PDF) between the different periods. This is done by showing the standard deviation of the PDFs from the individual periods (the standard deviation of the set of seven curves in Figure 6(a)). This shows that the decadal variations in the jet latitude PDF are largest at the latitudes of the peaks in the PDF. This is clear for the case of the northern peak of the PDF, but for the case of the southern peak the uncertainty across the ensemble is significant. This analysis provides some evidence that it is indeed changes in the occurrence of the three jet positions

© 2013 Royal Meteorological Society

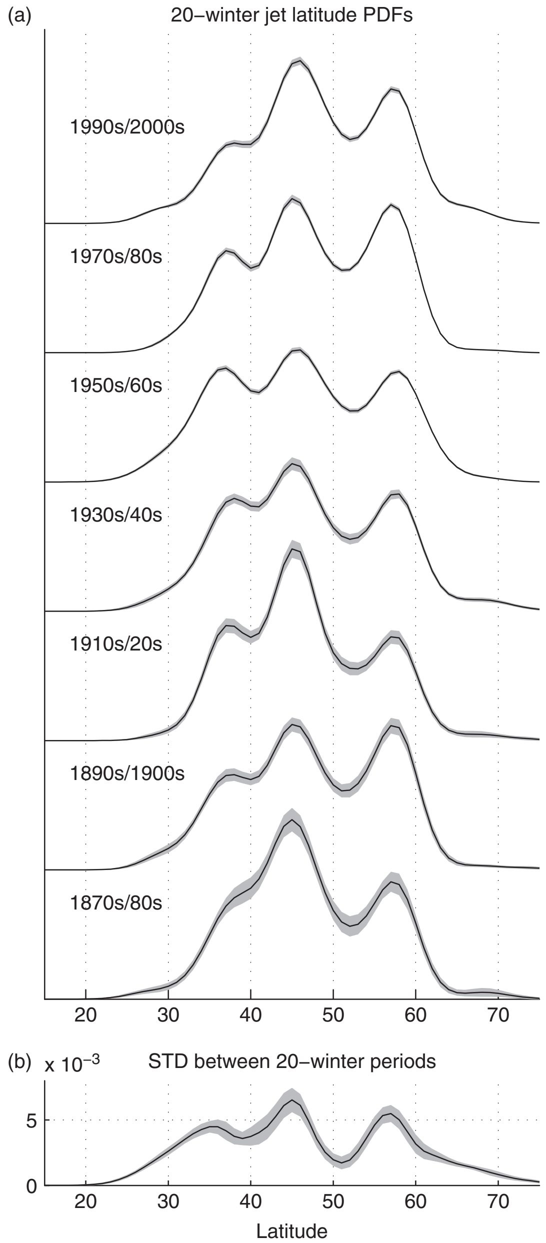

Figure 6. (a) PDFs of wintertime jet latitude constructed for 20 year periods by applying a kernel smoothing to the distributions as in Woollings *et al.* (2010a). (b) The line shows the ensemble mean of the standard deviation of the set of seven PDFs in panel (a), in units of probability. In both panels, the shading indicates the ± 2 standard deviation range of the relevant quantity across the ensemble members.

that are dominating the decadal variability. The decadal-scale jet variability is discussed further in the next section.

In contrast, the distributions of jet speed are all unimodal (not shown). However, the distributions are positively skewed for all months of the year, with skewness values between 0.1 and 0.7 (Czuchnicki, 2011). Since near-surface winds are used here, this could partly reflect the nonlinearities of boundary-layer drag, as described by Monahan (2006). In addition, some of the skewness in the seasonal distributions for the transition seasons of MAM and SON can be attributed to an artefact of the seasonal cycle. For example, the jet-speed distribution in MAM has a strong positive skew because the distribution in March is shifted towards stronger winds than in April and May, while the distributions for each of the individual months all have weaker skewness.

6. Long-term jet variability

In this section we further investigate the jet variability on interannual and decadal time-scales. Figure 7 shows time series of the seasonal mean jet latitude, formed by simply averaging the daily jet latitude values over the corresponding season. Firstly we note that the spread between ensemble members is relatively small, in particular in winter. This gives confidence that the observational coverage is dense enough to constrain the reanalysis even in the late 19th century. The ensemble spread is larger in the other seasons, which may reflect the weaker nature of large-scale pressure patterns so that surface-pressure observations provide weaker constraints on the general circulation. Despite this spread, there is clearly much agreement across the ensemble on many of the jet variations in the early period.

For comparison we have also derived the jet indices from the NCEP−NCAR reanalysis (Kalnay *et al.*, 1996) for the years since 1948 and these are shown in red in Figure 7. These indices are in extremely good agreement with the 20CR versions over this period, adding further confidence to the variability shown here.

In all seasons the range of interannual variability is of the order of 5−10°, so it is as large as the mean seasonal cycle. Strong multiyear variability is evident in all seasons, although weakest in autumn. Franzke and Woollings (2011) noted a positive trend in jet latitude over the ERA-40 period in an Empirical Mode Decomposition analysis that used data from all seasons. In agreement with this, Figure 7 shows positive jet latitude trends since 1960 in all seasons except autumn. However, these trends do not appear remarkable in the context of the longer records, and the jet latitude in recent decades has not exceeded values seen in earlier periods. The strong winter NAO trend from the 1960s to the 1990s does not appear so striking in terms of jet latitude in this longer record.

The corresponding time series of jet speed are shown in Figure 8. This time the NCEP−NCAR indices show some differences from the 20CR versions. Jet speeds are consistently slightly weaker in 20CR, for reasons that are unclear. However, the variability on both interannual and decadal time-scales shows close agreement between the two reanalyses. The series show considerable levels of low-frequency variability, with several instances of consecutive decades of anomalous values. As seen for jet latitude, the speed can exhibit year-to-year variations as large as the seasonal cycle. In some seasons the jet speed seems to have changed considerably over the first few decades of the reanalysis. While the ensemble spread again appears modest, these changes could reflect the drifting of the model back towards its own climatology in periods of sparse observations, as described in section 3. As for jet latitude, the recent few decades are not unusual in the long-term context. In particular, there is no evidence by this measure of a weakening in the summertime westerlies as suggested by Francis and Vavrus (2012) to have arisen from enhanced Arctic warming.

Trend analyses have been performed on the indices using the Empirical Mode Decomposition method, as in Franzke and Woollings (2011). This method defines the trend as the residual after all empirical oscillations have been removed from the time series. Note that the method is applied to the continuous daily time series and so cannot distinguish between different seasons. This analysis finds that the jet latitude exhibits a positive trend in every ensemble member that is significant at the 97.5% level. The mean poleward shift is 2.8° over the whole period or about 0.2° per decade. This is small compared with the interannual/decadal variability but still statistically significant. The trend (not shown) is close to linear over the whole period and it is not clear whether this trend reflects a response to external forcing such as greenhouse gas emissions or changes in slow climate components like the ocean. Artificial trends in the reanalysis associated with changes in observational coverage could play a role. In contrast, none of the ensemble members shows a significant trend in jet speed.

As in the ERA-40 analysis of Woollings and Blackburn (2012), the time series of jet latitude and speed are not significantly correlated (for example the winter series have a correlation of −0.07). While patterns of variability such as the NAO combine

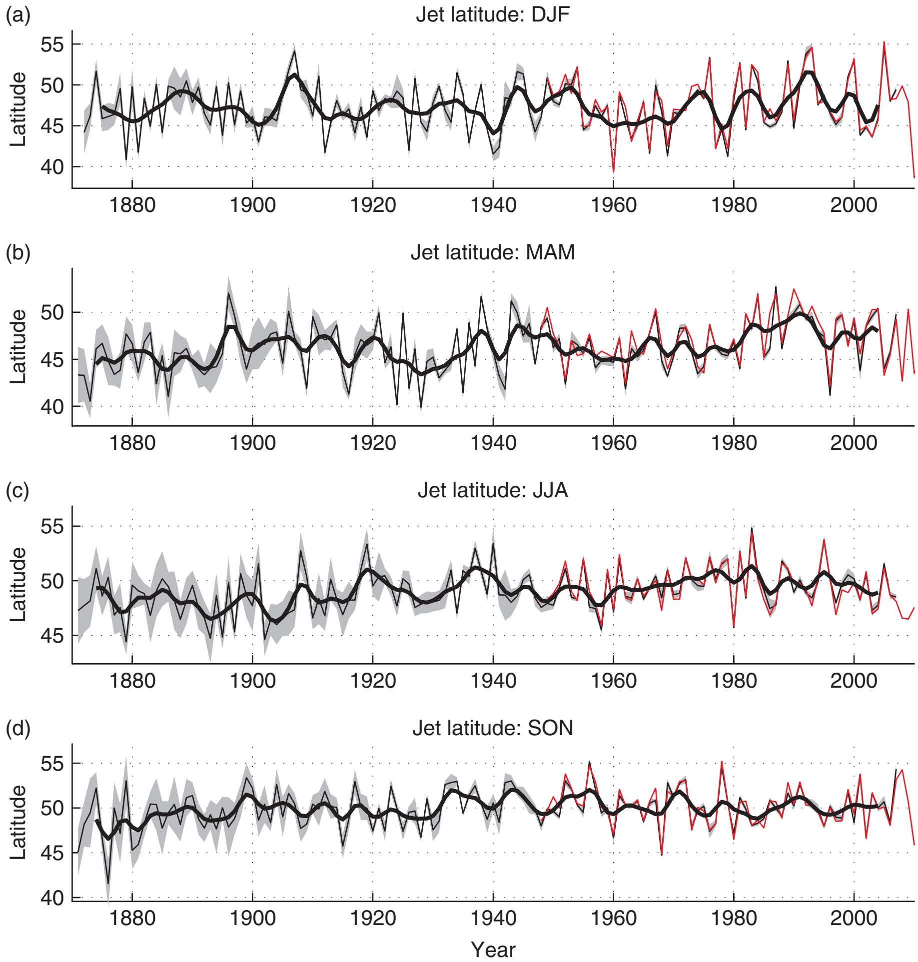

Figure 7. Time series of seasonal mean jet latitude, with the ±2 standard deviation range across the ensemble shaded. The thick lines show versions that have been smoothed with a 7 point binomial filter, which strongly damps time-scales shorter than 5 years. Red lines indicate indices derived from the NCEP–NCAR reanalysis in recent decades. This figure is available in colour online at wileyonlinelibrary.com/journal/qj

variations in jet latitude and speed, it seems that their variability is quite different and so they may be influenced by different factors. This is also supported by the clearly different seasonal cycles shown in section 4.

Example winter and summer power spectra of the seasonal time series are shown in Figure 9. In general the spectra are flat and so are similar to that of a white-noise process. The theoretical spectra for the equivalent red-noise process has been calculated from the seasonal mean data, using the lag one-year autocorrelation. This was found to be very similar to the white-noise spectra due to the weak autocorrelation in these series, so only the white-noise spectra are shown. Given the variability in regime occurrence shown in Figure 6, it is interesting that the wintertime jet latitude spectra in Figure 9 do not show strong variability at very low frequencies. For jet speed in particular, however, some of the spectra do show high power at the lowest frequencies, consistent with the impression of high multi-decadal variability in the time series of Figure 8.

To test the significance of the low-frequency power, we have calculated the 95% threshold that any individual spectral peak has to cross in order to be inconsistent with the noise model, allowing for multiplicity (Wilks, 2011). This is shown as a dashed line, which indicates that only the wintertime jet speed exhibits a significant spectral peak at low frequencies. To test for generally elevated power at low frequencies, we have adopted a Monte Carlo approach, generating 1000 time series of white noise with the same variance as each of the observed series. We then test how many of these surrogate time series have as much low-frequency variability as the observations. Here we define low-frequency variability simply as the variance of the 5 year and decadal means of the series. Table 1 shows the p values for the observed level of variability to occur in the simulated time series. This analysis suggests that the low-frequency variability of the jet speed is significantly higher than expected from white noise in all seasons apart from summer. Conversely, the low-frequency variability of the jet latitude is only significantly different from white noise in summer (and possibly in spring). These deviations from white-noise behaviour suggest that there is a role for influences outside the atmospheric dynamics to influence the jet on decadal time-scales.

Table 1. List of p values for the magnitude of the variability in 5 or 10 year means compared with an AR0 process. Values less than or equal to 0.05 are highlighted in bold.

Season	Jet latitude		Jet speed	
	5 years	10 years	5 years	10 years
DJF	0.34	0.19	**0.03**	**0.01**
MAM	0.08	**0.05**	**0.02**	**0.03**
JJA	**0.03**	**0.02**	0.28	0.07
SON	0.53	0.23	**0.01**	**0.002**

These conclusions are similar to those of Stephenson *et al.* (2000), who took a similar approach of analyzing a long record of a seasonal mean NAO index. Their study found that decadal NAO variations are significantly different from white noise at the 90% level and that the time series exhibits characteristics of long-range dependence. An alternative approach, not taken here, is to model the intraseasonal time-scale behaviour using a statistical model such as an AR1 process and then to perform Monte Carlo simulations to test the level of interannual–decadal variability that can occur just through sampling this short time-scale noise. Feldstein (2000a) showed that the observed Northern

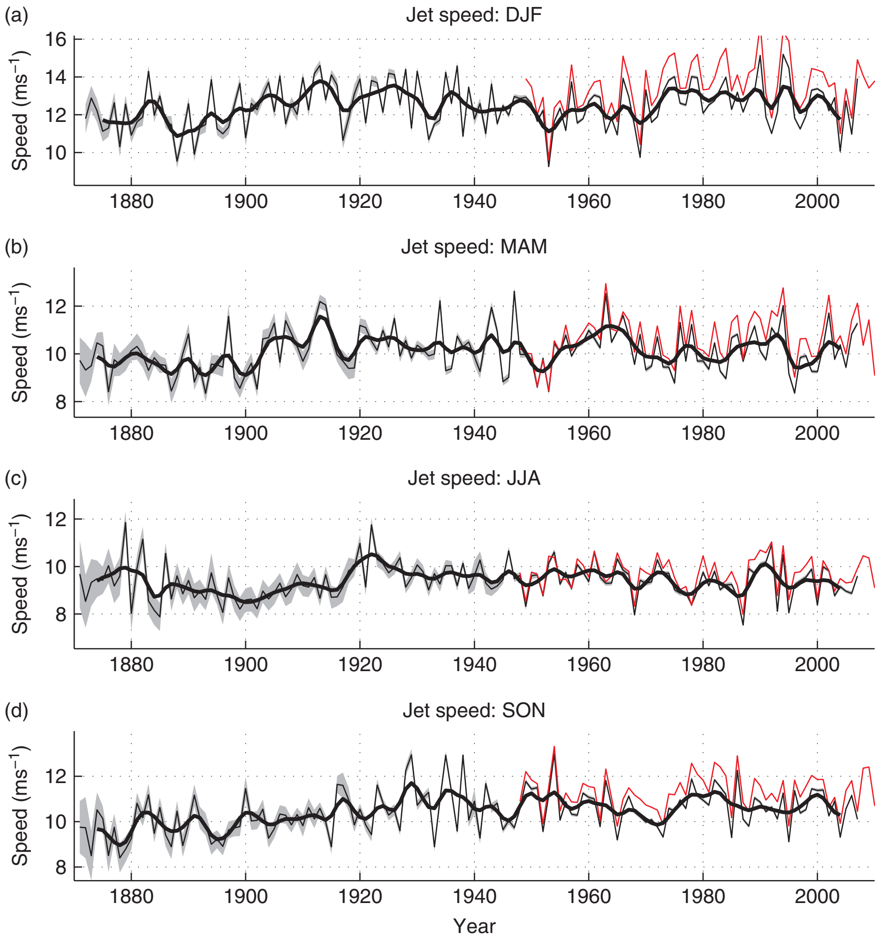

Figure 8. Time series of seasonal mean jet speed, with the ±2 standard deviation range across the ensemble shaded. The thick lines show versions that have been smoothed with a 7 point binomial filter. Red lines indicate indices derived from the NCEP–NCAR reanalysis in recent decades. This figure is available in colour online at wileyonlinelibrary.com/journal/qj

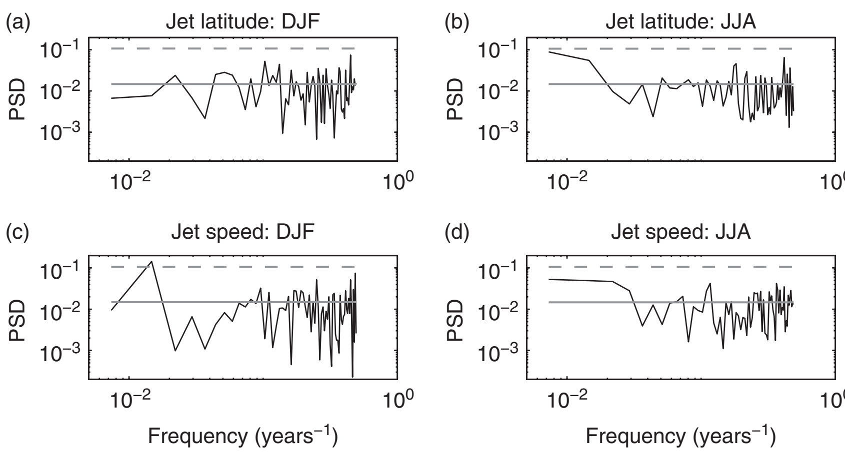

Figure 9. Example power spectra of the seasonal-mean jet latitude and speed. The spectra are computed for each ensemble member and the ensemble mean is plotted here. The ensemble mean of the theoretical spectra of the associated white-noise process is also plotted, with a dashed line indicating the 95% confidence level for any particular peak.

Hemisphere Zonal Index (related to the NAO) is not inconsistent with this 'climate noise' paradigm, although a relatively short 23 year period was used. Franzke and Woollings (2011) used a similar approach on the ERA-40 reanalysis data and concluded that around half of the interannual variability in the jet latitude index could be explained by climate noise.

In conclusion to this section, we note a somewhat counter-intuitive finding, particularly in winter. The decadal variability of the jet latitude seems to reflect regime behaviour comprising variations in the occurrence of the different preferred jet positions. Despite this, it is the jet speed which exhibits particularly strong decadal variability, while the time series of winter mean jet latitude is not distinguishable from white noise in this analysis.

7. Changes in intraseasonal variability

Häkkinen *et al.* (2011) recently analyzed wintertime atmospheric blocking in the Twentieth Century Reanalysis and suggested that the occurence of Euro–Atlantic blocking has varied on decadal time-scales in phase with the Atlantic Multidecadal Oscillation (AMO). A novel feature of their analysis is that blocking events all across the Atlantic and Europe are combined into one time series of occurrence. This process combines, for example, periods when the jet is displaced south of a Greenland block (Scherrer *et al.*, 2006; Croci-Maspoli *et al.*, 2007; Woollings *et al.*, 2008) with periods when the jet is displaced north of an Iberian block (Woollings *et al.*, 2011; Davini *et al.*, 2012). In this way, a period

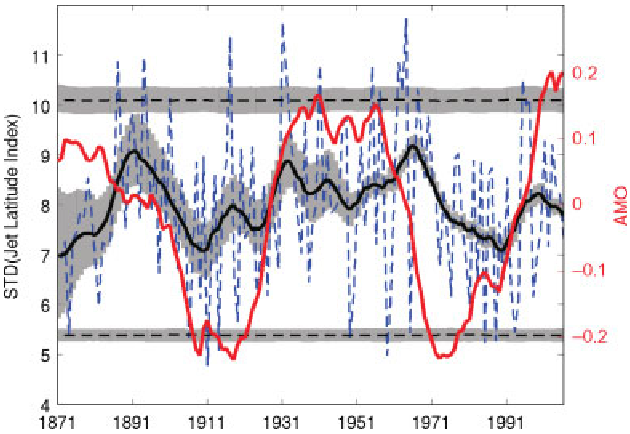

Figure 10. Time series of the standard deviation of jet latitude (in degrees) within each 90 day winter season. The blue dashed line indicates the ensemble mean. The black line shows the standard deviation of jet latitude smoothed with an 11 point Gaussian filter to isolate the decadal variations, with the 5th and 95th percentile range across the ensemble shown by shading. Dashed lines and associated shading mark the ensemble mean and the 5th and 95th percentile range of the 11 year smoothed ARMA simulations. Also plotted in red is a smoothed version of the AMO index smoothed with an 11 point Gaussian filter. This figure is available in colour online at wileyonlinelibrary.com/journal/qj

of enhanced blocking in their analysis could correspond to a period of strong intraseasonal variability in jet latitude.

Motivated by this, we show in Figure 10 the time series of intraseasonal jet latitude variability, defined as the standard deviation of the daily jet latitude values in each individual season. As anticipated, this time series shows considerable long-term changes in intraseasonal variability, with some similarity to the variations in blocking described by Häkkinen *et al.* (their figure 2(b)). The decadal changes are larger than the ensemble spread for much of the time series (see also Figure 1(b), which shows the ensemble spread of the unfiltered series). This suggests relatively low observational uncertainty in this variability, a factor that was not addressed by Häkkinen *et al.* There is also some similarity to the AMO variations, which are shown in red, although the two diverge, in particular in the 1870s and 1960s. The two smoothed time series only have a weak correlation of 0.19, so there is not a clear relationship between them. Ideally, of course, even longer records should be used to evaluate the correlation of variations on this time-scale.

Given the weak correlation, the aim of this section is not to suggest a relation between the AMO and the jet variability. Instead the aim is to investigate the origin of decadal variations in jet variability. Could these have arisen from climate noise (Feldstein, 2000b; Czaja *et al.*, 2003; Franzke, 2009) or are they reliant on some form of external forcing? To investigate this issue we compare the observations with a simple statistical model representing jet latitude fluctuations. In this case we use an Autoregressive Moving Average (ARMA) model for the winter season (December through February) as described by Franzke and Woollings (2011). The best-fitting ARMA model has been determined separately for the jet latitude in each ensemble member. These ARMA models are then integrated to give 1000 synthetic time series for each ensemble member from which time series of intraseasonal variability can be derived. The synthetic time series allow us to compute seasonal standard deviations of the fluctuations for each ensemble member separately. We then use the 5th and 95th percentiles of the standard deviations to gauge whether the observed interannual jet latitude fluctuations are consistent with the fluctuations generated by the ARMA model. The order of the ARMA model varies from about 3 to 10 amongst the ensemble members. It is not clear whether this is due to uncertainty in the model selection procedure or differences in the reanalysis realizations. However, the Monte Carlo approach is designed to take account of this uncertainty.

Figure 10 shows the results of this analysis. In order to focus on decadal scale variability, the time series has been smoothed with an 11 point Gaussian filter, which has a sharp cut-off in response at about 10 years. The observed decadal variations in intraseasonal variability (solid line) is almost always within the bounds of the decadal variability seen in the ARMA ensemble (dashed lines), showing that this level of decadal variability can arise without the need for memory in the system beyond a few days. This memory, as measured by the order of the ARMA process, is not longer than the typical life cycle of teleconnection patterns (Feldstein, 2000b; Franzke and Feldstein, 2005) or blocking (Tyrlis and Hoskins, 2008). Though we cannot prove that there were no external influences, our Monte Carlo results suggest that external forcing is not required to explain this variability. If the atmospheric variability does influence the ocean circulation, as proposed in Häkkinen *et al.* (2011), then this influence could comprise the ocean acting as an integrator of stochastic atmospheric forcing containing all time-scales, as in Hasselmann (1976) and Frankignoul and Hasselmann (1977).

8. Conclusions

We have used the Twentieth Century Reanalysis to derive a long record of variations in the latitude and speed of the North Atlantic eddy-driven jet. This reanalysis product allows some estimation of the circulation uncertainty due to the provision of multiple ensemble members. In the North Atlantic, the jet characteristics are well constrained by the available observations over the 20th century and show reasonable agreement in the late 19th century, in particular in winter. This is often not the case in other regions. Specific conclusions derived from this record are listed below.

- Both the latitude and speed of the jet have shown multi-year/decadal variability over the length of the 20th century in all seasons. The changes over the most recent few decades do not appear unusual compared with previous variations and recent values of these indices are not unprecedented in the historical record.
- The seasonal cycle of jet latitude, in particular, is quite modest compared with the large amount of variability on monthly/seasonal time-scales.
- The latitude and speed of the jet are not correlated in their interannual variability and they exhibit quite different seasonal cycles. This suggests that they may have quite different dynamical influences.
- The trimodal distribution of jet latitude in winter is a robust feature of this longer reanalysis and there is also evidence of similar preferred jet positions in the transition seasons. The related strong skewness of the NAO index is also seen in this long dataset.
- While general features of the jet statistics are robust, there can be significant differences between periods of as long as 40 years in features such as the mean jet speed, the detailed shape of the jet latitude PDF and the apparent structure in the seasonal cycle. This high level of variability suggests that long time periods may be needed for precise evaluations of climate models.
- There is some evidence that decadal variability in jet latitude is associated with changes in the occurrence of the different jet positions, although the uncertainty across the ensemble is large, in particular for variations of the southern peak. Despite this, it is the jet speed rather than latitude that has strong decadal variability, clearly different from a white-noise process.
- The level of wintertime intraseasonal variability in jet latitude has itself varied on decadal time-scales. However, these variations are not inconsistent with the variability exhibited by a simple statistical noise model with a memory of only a few days.

Acknowledgements

Support for the Twentieth Century Reanalysis Project dataset is provided by the US Department of Energy, Office of Science Innovative and Novel Computational Impact on Theory and Experiment (DOE INCITE) program and Office of Biological and Environmental Research (BER), and by the National Oceanic and Atmospheric Administration Climate Program Office. NCEP Reanalysis data provided by the NOAA/OAR/ESRL PSD, Boulder, Colorado, USA, from their web site at http://www.esrl.noaa.gov/psd/.

References

Archer CL, Caldeira K. 2008. Historical trends in the jet streams. *Geophys. Res. Lett.* **35**: l08 803. 10.1029/2008GL033614.

Athanasiadis PJ, Wallace JM, Wettstein JJ. 2010. Patterns of wintertime jet stream variability and their relation to the storm tracks. *J. Atmos. Sci.* **67**: 1361–1381. DOI: 10.1175/2009JAS3270.1.

Cattiaux J, Vautard R, Cassou C, Yiou P, Masson-Delmotte V, Codron F. 2010. Winter 2010 in Europe: A cold extreme in a warming climate. *Geophys. Res. Lett.* **37**: L20 704. 10.1029/2010GL044613.

Cohen J, Barlow M. 2005. The NAO, the AO, and global warming: How closely related? *J. Climate* **18**: 4498–4513.

Compo GP, Whitaker JS, Sardeshmukh PD, Matsui N, Allan RJ, Yin X, Gleason BE, Vose RS, Rutledge G, Bessemoulin P, Brönnimann S, Brunet M, Crouthamel RI, Grant AN, Groisman PY, Jones PD, Kruk MC, Kruger AC, Marshall GJ, Maugeri M, Mok HY, Nordli Ø, Ross TF, Trigo RM, Wang XL, Woodruff SD, Worley SJ. 2011. The Twentieth Century Reanalysis Project. *Q. J. R. Meteorol. Soc.* **137**: 1–28. DOI: 10.1002/qj.776.

Croci-Maspoli M, Schwierz C, Davies H. 2007. Atmospheric blocking – Space–time links to the NAO and PNA. *Clim. Dyn.* **29**: 713–725.

Czaja A, Robertson AW, Huck T. 2003. The role of Atlantic ocean–atmosphere coupling in affecting North Atlantic Oscillation variability. In *The North Atlantic Oscillation: Climatic Significance and Environmental Impact*, Hurrell J, Kushnir Y, Ottersen G, Visbeck M (eds). *Geophys. Monogr. Ser.* **134**: 147–172. AGU: Washington, DC.

Czuchnicki C. 2011. '*Seasonality of the eddy-driven jet stream variability and change*', Master's thesis. Dept. of Meteorology, University of Reading: Reading, UK.

Davini P, Cagnazzo C, Gualdi S, Navarra A. 2012. Bidimensional diagnostics, variability and trends of Northern Hemisphere blocking. *J. Climate*. **25**(19): 6496–6509.

Feldstein SB. 2000a. Is interannual zonal mean flow variability simply climate noise? *J. Climate* **13**: 2356–2362.

Feldstein SB. 2000b. The timescale, power spectra, and climate noise properties of teleconnection patterns. *J. Climate* **13**: 4430–4440.

Francis JA, Vavrus SJ. 2012. Evidence linking Arctic amplification to extreme weather in mid-latitudes. *Geophys. Res. Lett.* **39**: L06 801.

Frankignoul C, Hasselmann K. 1977. Stochastic climate models, Part II. Application to sea-surface temperature anomalies and thermocline variability. *Tellus* **29**: 289.

Franzke C. 2009. Multi-scale analysis of teleconnection indices: climate noise and nonlinear trend analysis. *Nonlinear Processes in Geophysics* **16**: 65–76.

Franzke C, Feldstein SB, 2005. The Continuum and Dynamics of Northern Hemisphere Teleconnection Patterns. *J. Atmos. Sci.* **68**: 3250–3267.

Franzke C, Woollings T. 2011. On the persistence and predictability properties of North Atlantic climate variability. *J. Climate* **24**: 466–472.

Franzke C, Woollings T, Martius O. 2011. Persistent circulation regimes and preferred regime transitions in the North Atlantic. *J. Atmos. Sci.* **68**: 2809–2825. DOI: 10.1175/JAS-D-11-046.1.

Häkkinen S, Rhines PB, Worthen DL. 2011. Atmospheric blocking and Atlantic multidecadal ocean variability. *Science* **334**: 655–659. DOI: 10.1126/science.1205683.

Hannachi A, Woollings T, Fraedrich K. 2012. The North Atlantic jet stream: a look at preferred positions, paths and transitions. *Q. J. R. Meteorol. Soc.* **138**: 862–877. DOI: 10.1002/qj.959.

Hasselmann K. 1976. Stochastic climate models, Part I, Theory. *Tellus* **28**: 473.

Hurrell JW. 1995. Decadal trends in the North Atlantic Oscillation: Regional temperatures and precipitation. *Science* **269**: 676–679.

Hurrell JW, Deser C. 2009. North Atlantic climate variability: The role of the North Atlantic Oscillation. *J. Marine Systems* **78**: 28–41.

Jones PD, Jonsson T, Wheeler D. 1997. Extension to the North Atlantic oscillation using early instrumental pressure observations from Gibraltar and south-west Iceland. *Int. J. Climatol.* **17**: 1433–1450. DOI: 10.1002/(SICI)1097-0088(19971115)17:13<1433::AID-JOC203>3.3.CO;2-G.

Kalnay E, Kanamitsu M, Kistler R, Collins W, Deaven D, Gandin L, Iredell M, Saha S, White G, Woollen J, Zhu Y, Leetmaa A, Reynolds B, Chelliah M, Ebisuzaki W, Higgins W, Janowiak J, Mo KC, Ropelewski C, Wang J, Jenne R and Joseph D. The NCEP/NCAR 40-year reanalysis project. *Bull. Am. Meteorol. Soc.* **77**: 437–471.

Koch P, Wernli H, Davies HC. 2006. An event-based jet-stream climatology and typology. *Int. J. Climatol.* **26**: 283–301. DOI: 10.1002/joc.1255.

Limbach S, Schömer E, Wernli H. 2012. Detection, tracking and event localization of jet stream features in 4-D atmospheric data. *Geoscientific Model Development* **5**: 457–470. DOI: 10.5194/gmd-5-457-2012.

Luterbacher J, Xoplaki E, Dietrich D, Jones PD, Davies TD, Portis D, Gonzalez-Rouco JF, von Storch H, Gyalistras D, Casty C, Wanner H. 2001. Extending North Atlantic Oscillation reconstructions back to 1500. *Atmos. Sci. Lett.* **2**: 114–124. DOI: 10.1006/asle.2002.0047.

Monahan AH. 2006. The probability distribution of sea surface wind speeds. Part I: Theory and seawinds observations. *J. Climate* **19**: 497–519. DOI: 10.1175/JCLI3640.1.

Osprey SM, Ambaum MHP. 2011. Evidence for the chaotic origin of Northern Annular Mode variability. *Geophys. Res. Lett.* **38**: L15702. DOI: 10.1029/2011GL048181.

Pinto JG, Raible CC. 2012. Past and recent changes in the North Atlantic Oscillation. *WIREs Clim. Change* **3**: 79–90. DOI: 10.1002/wcc.150.

Scherrer SC, Croci-Maspoli M, Schwierz C, Appenzeller C. 2006. Two-dimensional indices of atmospheric blocking and their statistical relationship with winter climate patterns in the Euro-Atlantic region. *Int. J. Climatol.* **26**: 233–249.

Stephenson DB, Pavan V, Bojariu R. 2000. Is the North Atlantic Oscillation a random walk? *Int. J. Climatol.* **20**: 1–18.

Strong C, Davis RE. 2007. Winter jet stream trends over the Northern Hemisphere. *Q. J. R. Meteorol. Soc.* **133**: 2109–2115.

Strong C, Davis RE. 2008. Variability in the position and strength of winter jet stream cores related to Northern Hemisphere teleconnections. *J. Climate* **21**: 584–592. DOI: 10.1175/2007JCLI1723.1.

Thompson DWJ, Wallace JM. 2001. Regional climate impacts of the Northern Hemisphere Annular Mode. *Science* **293**: 85–89.

Tyrlis E, Hoskins BJ. 2008. Aspects of Northern Hemisphere atmospheric blocking climatology. *J. Atmos. Sci.* **65**: 1638–1652.

Wilks DS. 2011. *Statistical Methods in the Atmospheric Sciences*, vol. 100. Academic Press: New York.

Woollings T, Blackburn M. 2012. The North Atlantic jet stream under climate change, as described by the NAO and EA patterns. *J. Climate* **25**: 886–902.

Woollings TJ, Hoskins BJ, Blackburn M, Berrisford P. 2008. A new Rossby wave-breaking interpretation of the North Atlantic Oscillation. *J. Atmos. Sci.* **65**: 609–626.

Woollings T, Hannachi A, Hoskins B. 2010a. Variability of the North Atlantic eddy-driven jet stream. *Q. J. R. Meteorol. Soc.* **649**: 856–868.

Woollings T, Hannachi A, Hoskins B, Turner A. 2010b. A regime view of the North Atlantic Oscillation and its response to anthropogenic forcing. *J. Climate* **23**: 1291–1307.

Woollings T, Pinto JG, Santos JA. 2011. Dynamical evolution of North Atlantic ridges and poleward jet stream displacements. *J. Atmos. Sci.* **68**: 954–963. DOI: 10.1175/2011JAS3661.1.

© 2013 Royal Meteorological Society